Towards enzyme-like enantioselectivity in the gas phase: conformational control of selectivity in chiral macrocyclic dimers†

Caterina Fraschetti, Marco Pierini, Claudio Villani,* Francesco Gasparrini, Stefano Levi Mortera and Maurizio Speranza*

Received (in Cambridge, UK) 6th May 2009, Accepted 13th July 2009
First published as an Advance Article on the web 31st July 2009
DOI: 10.1039/b909017g

Conformational factors in self-assembled chiral tetraamide macrocycles control their gas-phase enantioselectivity towards the ethyl ester of naphthylalanine to levels typical of enzymes.

Enzymes are proteic macromolecules that enable and support life functions. A key feature of enzymes is their capability for "molecular recognition". Size- and shape-specific non-covalent interactions, assisted by extensive desolvation phenomena,[1] allow the selective absorption of the target molecule into the enzyme structure and its modification at the "active site".[2–5]

$$[(M^S)_n\bullet H\bullet A^S]^+ \xrightarrow[+B^R\text{-}A^S]{k^R_{homo}} [(M^S)_n\bullet H\bullet B^R]^+ \quad (1a)$$
$$\xrightarrow[+B^S\text{-}A^S]{k^S_{homo}} [(M^S)_n\bullet H\bullet B^S]^+$$

$$[(M^R)_n\bullet H\bullet A^S]^+ \xrightarrow[+B^R\text{-}A^S]{k^R_{hetero}} [(M^R)_n\bullet H\bullet B^R]^+ \quad (1b)$$
$$\xrightarrow[+B^S\text{-}A^S]{k^S_{hetero}} [(M^R)_n\bullet H\bullet B^S]^+$$

The amazing selectivity and catalytic proficiency of enzymes have provided chemists with a stimulus to design "synthetic enzymes" for understanding the mechanism of action of enzymes and for attempting to reproduce them for practical applications. However, these synthetic receptors exhibit selectivities which are orders of magnitude lower than those of enzymes, even when acting in the gas phase, *i.e.* under conditions reproducing the extensive desolvation undergone by the target molecule when entering the enzyme cavity.[6]

The chiral macrocycles $M^{R/S}$ of Chart 1 are synthetic receptors that gained some attention in recent gas-phase studies.[7,8] Their gas-phase enantioselectivity towards the several amino acid derivatives, including the ethyl ester of (*S*)-naphthylalanine (A^S), was evaluated by generating the proton-bonded $[M^{R/S}\cdot H\cdot A^S]^+$ adducts in the cell of a Fourier-transform ion cyclotron resonance mass spectrometer (FT-ICR-MS), equipped with an electrospray ionization source (ESI), and by measuring their reaction kinetics toward either (*R*)-(−)-(B^R) or (*S*)-(+)-2-butylamine (B^S) QJ;(see ESI†). The reaction enantioselectivity is defined by the $\rho^R = k^R_{homo}/k^R_{hetero}$ and $\rho^S = k^S_{homo}/k^S_{hetero}$ ratios, when referred to the configuration of M, or by the $\xi_{homo} = k^R_{homo}/k^S_{homo}$ and $\xi_{hetero} = k^R_{hetero}/k^S_{hetero}$ ratios, when referred to the configuration of the amine B (eqn (1a,b)).

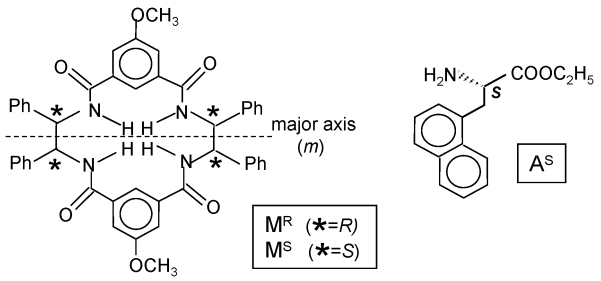

Chart 1 Formulae of the chiral tetraamidic receptors $M^{R/S}$ and of the ethyl ester of (S)-naphthylalanine A^S.

Reactions (1a,b) ($n = 1$), involving the two-body $[M^{R/S}\cdot H\cdot A^S]^+$ complexes, exhibit enantioselectivities (ρ = *ca.* 0.05) among the largest ever measured in the gas phase, that were attributed to differences in the structure and the relative stability of the $[M^{R/S}\cdot H\cdot A^S]^+$ diastereoisomers.[8] Indeed, molecular mechanics (MM) calculations indicate that macrocycles $M^{R/S}$ may assume diverse stable conformations, as illustrated in Chart 2. In both eq–eq and ax–ax geometries, macrocycles $M^{R/S}$ have C_2-symmetric folded structures with a concave face F1 and a convex one F2. The eq–eq conformers, by far the most stable ones in the isolated $M^{R/S}$ molecules, acquire in the gas phase a different conformation by induced fit on complexation with some amino acid derivatives, like A^S. This leads to the co-existence in the gas phase of stable eq–eq and ax–ax structures, in proportions depending on the configuration of $M^{R/S}$ and characterized by different stability and reactivity towards the 2-aminobutane enantiomers. In this case, reactions (1a,b) ($n = 1$) obey bi-exponential kinetics.

Despite its unusually large ρ value, the gas-phase enantioselectivity of $[M^{R/S}\cdot H\cdot A^S]^+$ towards $B^{R/S}$ is still well below

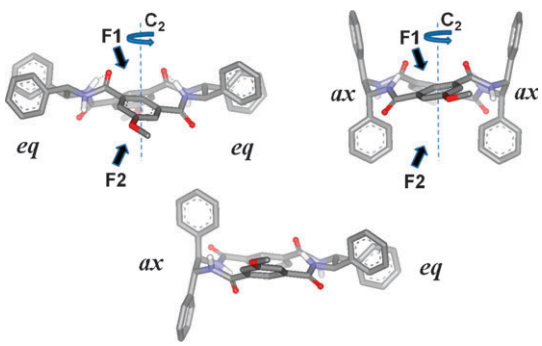

Chart 2 Relevant minimum energy structures of the M^R host found by conformational search.

Dipartimento di Chimica e Tecnologie del Farmaco, Università di Roma "La Sapienza", Rome, Italy. E-mail: maurizio.speranza@ uniroma1.it; Fax: +39-06-49913497; Tel: +39-06-49913602

† Electronic supplementary information (ESI) available: ESI-FT-ICR experimental and MM computational details. Kinetic plots. See DOI:10.1039/b909017g

Table 1 Rate constants for the B-induced loss of A^S from the diastereomeric $[(M^{R/S})_2{\cdot}H{\cdot}A^S]^+$ complexes

		B^R = (*R*)-(−)-$C_4H_9NH_2$			B^S = (*S*)-(+)-$C_4H_9NH_2$			
Complex	%	k^R [a]	eff = $100k^R/k_C$ [b]	$\rho^R = k^R_{homo}/k^R_{hetero}$	k^S [a]	eff = $100k^S/k_C$ [b]	$\rho^S = k^S_{homo}/k^S_{hetero}$	ξ [c]
$[(M^S)_2{\cdot}H{\cdot}A^S]^+$	—	0.62 ± 0.03	0.6	0.015 ± 0.002	0.73 ± 0.02	0.7	0.016 ± 0.001	ξ_{homo} = 0.86 ± 0.06
$[(M^R)_2{\cdot}H{\cdot}A^S]^+_{fast}$	13 ± 1	40.7 ± 1.6	37		45.5 ± 2.2	41		ξ_{hetero} = 0.89 ± 0.05
$[(M^S)_2{\cdot}H{\cdot}A^S]^+$	—	0.62 ± 0.03	0.6	0.17 ± 0.01	0.73 ± 0.02	0.7	0.23 ± 0.01	ξ_{homo} = 0.86 ± 0.06
$[(M^R)_2{\cdot}H{\cdot}A^S]^+_{slow}$	87 ± 1	3.62 ± 0.15	3.3		3.20 ± 0.18	2.9		ξ_{hetero} = 1.13 ± 0.08

[a] $k \times 10^{11}$ cm^3 per molecule per second. [b] Reaction efficiency expressed as the ratio between the measured rate constants k and the corresponding collision constant k_C, calculated using the trajectory calculation method.[11] [c] See text.

that typical of enzymes. In this communication, kinetic results are presented which demonstrate how conformational effects in self-assembled hosts $M^{R/S}$ may control their gas-phase enantioselectivity towards A^S to levels comparable to, if not higher than, those of many enzymes.[9]

Table 1 reports the second-order rate constants of reactions (1a,b) (n = 2) between the three-body $[(M^{R/S})_2{\cdot}H{\cdot}A^S]^+$ complexes and $B^{R/S}$, as well as the relevant enantioselectivity factors ρ^R, ρ^S, ξ_{homo}, and ξ_{hetero}. Likewise the two-body $[M^{R/S}{\cdot}H{\cdot}A^S]^+$ complexes, their three-body $[(M^R)_2{\cdot}H{\cdot}A^S]^+$ homologue exhibits bi-exponential kinetics pointing to the occurrence of two stable structures, $[(M^R)_2{\cdot}H{\cdot}A^S]^+_{fast}$ and $[(M^R)_2{\cdot}H{\cdot}A^S]^+_{slow}$, characterized by different reactivity towards $B^{R/S}$. In contrast, the homochiral $[(M^S)_2{\cdot}H{\cdot}A^S]^+$ complex displays mono-exponential kinetics which suggests the occurrence of a single structure or, alternatively, of several ones but with comparable reactivity towards $B^{R/S}$. Relative to the homochiral $[(M^S)_2{\cdot}H{\cdot}A^S]^+$complex, the heterochiral $[(M^R)_2{\cdot}H{\cdot}A^S]^+_{slow}$structure reacts from 4.4 to 5.8 times faster (ρ^R = 0.17 ± 0.01; ρ^S = 0.23 ± 0.01), whereas the $[(M^R)_2{\cdot}H{\cdot}A^S]^+_{fast}$one reacts from 62 to 66 times faster (ρ^R = 0.015 ± 0.002; ρ^S = 0.016 ± 0.001). The latter ρ values clearly highlight a gas-phase enantioselectivity (corresponding to an ee of *ca.* 97% in a single reactive event) comparable to that of many enzymes. A comparison of the ρ values of the two-body $[M^{R/S}{\cdot}H{\cdot}A^S]^+$ complexes and their three-body $[(M^{R/S})_2{\cdot}H{\cdot}A^S]^+$ counterparts is given in Table 2. Its inspection reveals that self-assembling of hosts $M^{R/S}$ does produce a significant effect on the reaction enantioselectivity which decreases with the *slow* components of the reaction and increases with the *fast* ones.

To understand the factors determining such a behavior, an in-depth theoretical study has been undertaken by performing extensive "quasi-flexible" multiconformational molecular dockings based on molecular mechanics calculations (see ESI,† p. S7).[10] The most representative structures of the homochiral $[(M^S)_2{\cdot}H{\cdot}A^S]^+$ and the heterochiral $[(M^R)_2{\cdot}H{\cdot}A^S]^+$ aggregates can be conveniently clustered (within a 3 kcal mol^{-1} window) in two geometric typologies (**I** and **II** in Fig. 1). Both $\mathbf{I}_{hetero}$ and $\mathbf{I}_{homo}$ structures are characterized by several H-bonds between the $-NH_3^+$ group of the guest and the converging pairs of carbonyls on the convex sides F2 of two facing host molecules (Fig. S5, ESI†). In contrast, the $\mathbf{II}_{homo}$ and $\mathbf{II}_{hetero}$ aggregates are characterized by a minor number of H-bonds among the $-NH_3^+$ group of the guest and the converging pair of carbonyls placed on the convex sides F2 of only one host molecule (in blue in Fig. 1), with ax–ax geometry in $\mathbf{II}_{hetero}$ and eq–eq one in $\mathbf{II}_{homo}$. However, while in $\mathbf{II}_{homo}$, the second host molecule (in grey in Fig. 1) cannot directly interact with the guest, in $\mathbf{II}_{hetero}$ the second host molecule is in direct contact with ester A through a H-bond and an efficient C–H$\cdots\pi$ interaction (Fig. S5, ESI†). Interestingly, the dimer $(M)_2$ assumes a Y-shaped disposition with a C_2 symmetry in both $\mathbf{I}_{homo}$ and $\mathbf{I}_{hetero}$ complexes. In $\mathbf{II}_{homo}$, it shows a D_2 symmetry,[9] whereas in $\mathbf{II}_{hetero}$, it does not show any symmetry. The topological features of the most stable $\mathbf{I}_{homo}$ and $\mathbf{I}_{hetero}$ structures are reported in Fig. 2.

The energy of the simulated $[(M^{R/S})_2{\cdot}H{\cdot}A^S]^+$ complexes can be conveniently analyzed to attempt a rationalization of the relevant kinetic results of Table 2. On the grounds of the computed relative energy of the $\mathbf{I}_{hetero}$ and $\mathbf{II}_{hetero}$ isomers, the first structure is attributed to the less reactive $[(M^R)_2{\cdot}H{\cdot}A^S]^+_{slow}$ isomer and the latter to the more reactive $[(M^R)_2{\cdot}H{\cdot}A^S]^+_{fast}$ one. However, the experimental distribution of these two isomers (*fast*: 13 ± 1%; *slow*: 87 ± 1%, corresponding to a conformational stability difference of about 1.1 kcal mol^{-1} at 300 K; Table 1) is only in semiquantitative agreement with the calculated energy gap of 3.0 kcal mol^{-1} (Fig. 1). Furthermore, the observed mono-exponential kinetics of the reaction with the homochiral $[(M^S)_2{\cdot}H{\cdot}A^S]^+$ complex is inconsistent with the 1.2 kcal mol^{-1} difference between the calculated energies of $\mathbf{I}_{homo}$ and $\mathbf{II}_{homo}$,

Table 2 Comparison of the gas-phase enantioselectivities of the reaction of $[M^{R/S}{\cdot}H{\cdot}A^S]^+$ [a] and $[(M^{R/S})_2{\cdot}H{\cdot}A^S]^+$ towards B

		eff = $100k/k_C$ [b]					
Complex		homo	hetero	$\rho^R = k^R_{homo}/k^R_{hetero}$	$\rho^S = k^S_{homo}/k^S_{hetero}$	$\Delta\Delta G^{*}_{exp}$ [c]/kcal mol^{-1}	$\Delta\Delta H^{\circ}_{th}$ [d]/kcal mol^{-1}
$[M^{R/S}{\cdot}H{\cdot}A^S]^+$	fast	1	21	0.046 ± 0.004	0.050 ± 0.009	1.8 ± 0.1	1.0
	slow	0.05	1	0.052 ± 0.007	0.048 ± 0.009	1.8 ± 0.1	1.3
$[(M^{R/S})_2{\cdot}H{\cdot}A^S]^+$	fast	0.6	39	0.015 ± 0.002	0.016 ± 0.001	2.5 ± 0.1	2.7–3.9[e]
	slow	0.6	3.1	0.17 ± 0.01	0.23 ± 0.01	1.0 ± 0.1	0.9

[a] Ref. 8. [b] See footnote b in Table 1, $k = (k^R + k^S)/2$. [c] $\Delta\Delta G^{*}_{exp} = \Delta G^{*}_{homo} - \Delta G^{*}_{hetero} = -RT\ln(\rho^R + \rho^S)/2$, T = 300 K. [d] $\Delta\Delta H^{\circ}_{th} = \Delta H^{\circ}_{homo} - \Delta H^{\circ}_{hetero}$, calculated at T = 300 K. [e] Energy differences calculated between the stability of the single structures $\mathbf{I}_{homo}$ and $\mathbf{II}_{homo}$ and that of $\mathbf{II}_{hetero}$.

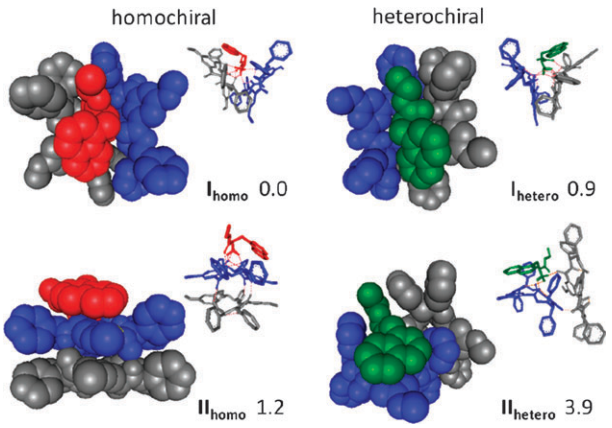

Fig. 1 Structures and relative energies (kcal mol^{-1}) of the most stable homochiral $[(M^R)_2{\cdot}H{\cdot}A^R]^+$ ($\mathbf{I}_{homo}$ and $\mathbf{II}_{homo}$) and heterochiral $[(M^R)_2{\cdot}H{\cdot}A^S]^+$ ($\mathbf{I}_{hetero}$ and $\mathbf{II}_{hetero}$) complexes. For the sake of clarity, hydrogen atoms are omitted with the exception of those bonded to nitrogen atoms.

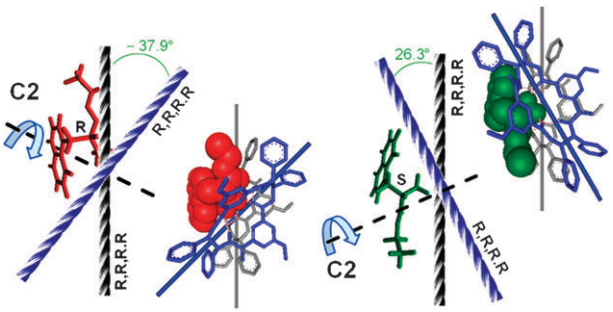

Fig. 2 Topological representation of $\mathbf{I}_{homo}$ (left) and $\mathbf{I}_{hetero}$ (right). The represented C_2 symmetry axes refer to the host dimer alone. The two spiral bars represent the major axis *m* of the two host molecules (Chart 1) in the corresponding structures. The $(M)_2$ supramolecules have a twisted structure, and the guest configuration controls their absolute sense of twist. Thus, the guest induces a left (−37°) and right (+26°) handed twist between the major axes *m* in the homo- and heterochiral three-body structures, respectively.

which would allow their co-existence in the gas phase. In this frame, the mono-exponential kinetics exhibited by $[(M^S)_2{\cdot}H{\cdot}A^S]^+$ can only be explained by admitting that $\mathbf{I}_{homo}$ and $\mathbf{II}_{homo}$ are endowed with a comparable reactivity towards B. Interestingly, this latter hypothesis finds a very persuasive support from the kinetic behavior already evidenced in the reactions (1a,b) ($n = 1$) with the two-body homochiral $[M^S{\cdot}H{\cdot}A^S]^+$ complex.[8] Indeed, a strict structural relationship exists between $\mathbf{II}_{homo}$ and its two-body $[M^S{\cdot}H{\cdot}A^S]^+_{fast}$ counterpart (Fig. S6, ESI†). Thus, the quite similar reaction efficiency exhibited by $\mathbf{I}_{homo}$ (average value: 0.6%, Table 2) and $[M^S{\cdot}H{\cdot}A^S]^+_{fast}$ (average value: 1.0%, Table 2) leaves one to retain that the same virtual equivalence must exist between the rate constants for the displacement processes involving $\mathbf{I}_{homo}$ and $\mathbf{II}_{homo}$. As reported in Table 2, an excellent correlation does exist between the experimental $\Delta\Delta G^*_{exp}$ (1.0 ± 0.1 kcal mol^{-1}) and the calculated $\Delta\Delta H^\circ_{th}$ difference (0.9 kcal mol^{-1}) of the low-energy $\mathbf{I}_{hetero}$ and $\mathbf{I}_{homo}$ structures. This correspondence suggests that the measured enantioselectivities are determined more by the relative stability of the diastereomeric $[(M^{R/S})_2{\cdot}H{\cdot}A^S]^+$ complexes than by that of the corresponding eqn (1a,b) transition structures.

As shown for the two-body $[M^{R/S}{\cdot}H{\cdot}A^S]^+$ complexes,[8] the comparable enantioselectivity exhibited by their *fast* and *slow* isomers (ρ_{fast} and ρ_{slow} *ca.* 0.050; Table 2) is attributed to the fact that the host assumes the same conformation, *i.e.* ax–ax in the most stable *slow* isomer and eq–eq in the less stable *fast* one. This means that the observed enantioselectivities are essentially determined by conformational factors, *i.e.* by changes in the intensity of non-covalent host–guest interactions as the host (or guest) configuration is inverted. A similar conclusion can be reached for the most stable three-body $\mathbf{I}_{homo}$ and $\mathbf{I}_{hetero}$ isomers (Fig. 1), wherein the two host molecules acquire the same eq–eq geometry. However, the differently distorted Y-shaped disposition of the eq–eq host molecules in $\mathbf{I}_{homo}$ and $\mathbf{I}_{hetero}$ (Fig. 2) decreases the reaction efficiency in general, but much less for the first (eff = 0.6 ($n = 2$); 1 ($n = 1$)) than for the latter (eff = 3.1 ($n = 2$); 21 ($n = 1$); Table 2). This obviously reduces the enantioselectivity of the reactions (1a,b) with $\mathbf{I}_{homo}$ and $\mathbf{I}_{hetero}$ (ρ'*s* of *ca.* 0.2) relative to that displayed by $[M^{R/S}{\cdot}H{\cdot}A^S]^+$ (ρ'*s* of *ca.* 0.05). In $\mathbf{II}_{hetero}$ (Fig. 1), instead, no tridimensional regularity is observed since one host molecule in the eq–eq conformation is facing the other in the ax–ax one. With this fully asymmetric disposition, the stabilizing π–π interactions in *slow* ax–ax $[M^R{\cdot}H{\cdot}A^S]^+$ isomer, between the naphthyl ring of A^S and the isophthalic rings of the host,[8] are partially destroyed in $\mathbf{II}_{hetero}$ by the presence of the second eq–eq host. The consequence is that the reaction efficiency increases 39 times (Table 2). This obviously enhances the enantioselectivity of the *fast* component of reactions (1a,b) relative to that displayed by $[M^{R/S}{\cdot}H{\cdot}A^S]^+$. It is concluded that the proton-bound $[(M^{R/S})_2{\cdot}H]^+$ dimer in the diastereomeric $[(M^{R/S})_2{\cdot}H{\cdot}A^S]^+$ complexes may act as gaseous enzyme mimics. Depending on the configuration of the amino acidic guest, the $[(M^{R/S})_2{\cdot}H]^+$ moiety adapts itself to maximize non-covalent interactions with the guest. Significant conformational changes take place in $[(M^{R/S})_2{\cdot}H]^+$ which confer to the diastereomeric $[(M^{R/S})_2{\cdot}H{\cdot}A^S]^+$ complexes a relatively large stability difference and, hence, an unprecedented thermodynamic enantioselectivity in their gas-phase reactions (1a,b) ($n = 2$).

Notes and references

1 F. Hollfelder, A. J. Kirby and D. S. Tawfik, *Nature*, 1996, **383**, 60–63.
2 J. M. Lehn, in *Supramolecular Chemistry. Concepts and Perspectives*, Wiley-VCH, Weinheim, 1995.
3 P. D. Beer, P. A. Gale and D. K. Smith, in *Supramolecular Chemistry (Oxford Chemistry Primers, 74)*, Oxford University Press, Oxford, 1999.
4 H. J. Schneider and A. Yatsimirsky, *Chem. Soc. Rev.*, 2008, **37**, 263–277.
5 J. W. Steed and J. L. Atwood, in *Supramolecular Chemistry*, Wiley, New York, 2000.
6 See, for instance: (*a*) M. Speranza, F. Gasparrini, B. Botta, C. Villani, D. Subissati, C. Fraschetti and F. Subrizi, *Chirality*, 2009, **21**, 69–86; (*b*) M. Speranza, *Int. J. Mass Spectrom.*, 2004, **232**, 277–317; (*c*) M. Speranza, *Adv. Phys. Org. Chem.*, 2004, **39**, 147–281; (*d*) C. Fraschetti, M. Aschi, A. Filippi, A. Giardini and M. Speranza, *Chem. Commun.*, 2008, 2544–2546.
7 A. Filippi, F. Gasparrini, M. Pierini, M. Speranza and C. Villani, *J. Am. Chem. Soc.*, 2005, **127**, 11912–11913.
8 F. Gasparrini, M. Pierini, C. Villani, A. Filippi and M. Speranza, *J. Am. Chem. Soc.*, 2008, **130**, 522–534.
9 P. F. Mugford, U. G. Wagner, Y. Jiang, K. Faber and R. J. Kazlauskas, *Angew. Chem., Int. Ed.*, 2008, **47**, 8782–8793.
10 C. Fraschetti, M. Pierini, C. Villani, F. Gasparrini, A. Filippi and M. Speranza, *Collect. Czech. Chem. Commun.*, 2009, **74**, 275–297.
11 T. Su and W. J. Chesnavitch, *J. Chem. Phys.*, 1982, **76**, 5183.

